NASA Technical Memorandum 106385
AIAA–95–0889

Axis Switching and Spreading of an Asymmetric Jet—Role of Vorticity Dynamics

K.B.M.Q. Zaman
Lewis Research Center
Cleveland, Ohio

Prepared for the
33rd Aerospace Sciences Meeting and Exhibit
sponsored by the American Institute of Aeronautics and Astronautics
Reno, Nevada, January 9–12, 1995

National Aeronautics and
Space Administration

AXIS SWITCHING AND SPREADING OF AN ASYMMETRIC JET -- ROLE OF VORTICITY DYNAMICS

by

K. B. M. Q. Zaman
NASA Lewis Research Center
Cleveland, OH 44135

Abstract

The effects of vortex generators and periodic excitation on vorticity dynamics and the phenomenon of axis switching in a free asymmetric jet are studied experimentally. Most of the data reported are for a 3:1 rectangular jet at a Reynolds number of 450,000 and a Mach number of 0.31. The vortex generators are in the form of 'delta tabs', triangular shaped protrusions into the flow, placed at the nozzle exit. With suitable placement of the tabs, axis switching could be either stopped or augmented. Two mechanisms are identified governing the phenomenon. One, as described by previous researchers and referred to here as the ω_θ-*induced dynamics*, is due to difference in induced velocities for different segments of a rolled up azimuthal vortical structure. The other, the ω_X-*induced dynamics*, is due to the induced velocities of streamwise vortex pairs in the flow. Both dynamics can be active in a natural asymmetric jet; the tendency for axis switching caused by the ω_θ-induced dynamics may be, depending on the streamwise vorticity distribution, either resisted or enhanced by the ω_X-induced dynamics. While this simple framework qualitatively explains the various observations made on axis switching, mechanisms actually in play may be much more complex. The two dynamics are not independent as the flow field is replete with both azimuthal and streamwise vortical structures which continually interact. Phase averaged flow field data for a periodically forced case, over a volume of the flow field, are presented and discussed in an effort to gain insight into the dynamics of these vortical structures.

1. Introduction

In a continuing effort to increase mixing in free shear flows, various methods of flow control are being explored in an experimental research program at NASA Lewis Research Center. The effect of passive, vortex generating 'tabs' has been explored over the past several years.[1,2] Tabs are protrusions into the flow placed at the jet nozzle exit. They produce large distortions in the jet which are accompanied by a significant increase in entrainment and spreading. While experimenting with asymmetric jets, it was observed that the tabs could not only affect mixing but also the phenomenon of axis switching in these jets. Depending on the number and placement, the tabs could either stop or promote the axis switching. These observations led to the present investigation.

Axis switching is a phenomenon in which the cross section of an asymmetric jet evolves in such a manner that, after a certain distance from the nozzle, the major and the minor axes are interchanged. Most previous studies involving rectangular or elliptic jets reported axis switching.[3-5] From available data,[6,7] it becomes apparent that the switching occurs not due to a helical turning of the jet column. Instead, the jet cross section expands in the direction of the minor axis and contracts in the direction of the major axis, and thereby a 90° switch takes place after a certain downstream distance. Typically, a first switchover is quite prominent and may take place a few equivalent diameters from the nozzle exit. A second, occurring much farther downstream, and even a third switchover have been observed;[8] but the latter switchovers are usually faint and may not be easily detectable.

Often the location of the switchover may be quite uncertain. Krothapalli *et al.*[5] compared their data on rectangular jets with previous results and showed that the distance of the first switchover from the nozzle increased with increasing aspect ratio of the nozzle. However, the uncertainty range was large; for example, the switchover location for a 10:1 aspect ratio jet was within a range of x/D = 25 to 65. Here, D denotes the equivalent diameter based on the nozzle exit area. The data evaluated by them covered larger aspect ratio nozzles but an extrapolation showed that the first switchover location for a smaller, 3:1 aspect ratio jet, for

example, could be anywhere from very close to the nozzle exit to as far downstream as x/D = 40.

In fact, even whether a switchover will occur or not with a given nozzle may be uncertain and depend on the flow condition. This is illustrated by the data in Fig. 1, taken in connection with a study of comparative mixing with various asymmetric nozzles. The data are for a small 3:1 rectangular nozzle with D = 1.47 cm. Figures 1(a) and (b) show that by x/D = 14 the jet cross section, at a subsonic condition, has become round and it stays that way farther downstream. There might be some mild undulations in the variations of the major and the minor axes but this is not significant. What is significant, and rather puzzling, is the fact that the same nozzle when run at a supersonic condition exhibits a clear axis switchover. This is illustrated in Figs. 1(c) and (d). Note that the nozzle major axis is aligned vertically as sketched in these figures. A clearer axis switchover at supersonic conditions, in contrast to subsonic conditions, was also observed with a 3:1 elliptic nozzle as well as a 8:1 rectangular nozzle.[9]

Gutmark & Schadow[10] had reported an interesting set of data on the flow from small aspect ratio slot nozzles. In the case where the nozzle was essentially an orifice, the jet went through a rapid axis switchover by x/D = 2. However, when a contraction section leading to the nozzle exit was added, the resulting jet diverged in the major axis plane over the measurement range of x/D = 10. Such a trend corroborates an earlier observation that the axis switchover occurs, "...further downstream for a jet exiting from a long channel than for a jet exiting from an orifice".[5] Hussain & Husain[8] further confirmed this difference between jets from an orifice nozzle and a nozzle with contraction.

The observations made in the foregoing bring up the question as to what determines the various trends. Why is there an axis switching in the supersonic condition of Fig. 1 but none in the subsonic condition? Why does the axis switching observed with an orifice nozzle stop when a contraction section is added? An explanation for axis switching in a jet has been given in Ref. 8. This explanation is based on the dynamics of rolled up azimuthal vortex structures (see also, Refs. 7, 11-16). This, referred to here as the ω_θ-*induced dynamics*, will be reviewed in the text. It will be reasoned that while this explains many of the observations, including the one made for the supersonic case, the effects of the tabs are not explained satisfactorily. The dynamics of streamwise vortex pairs occurring in an asymmetric jet are inferred to also play a significant role. In

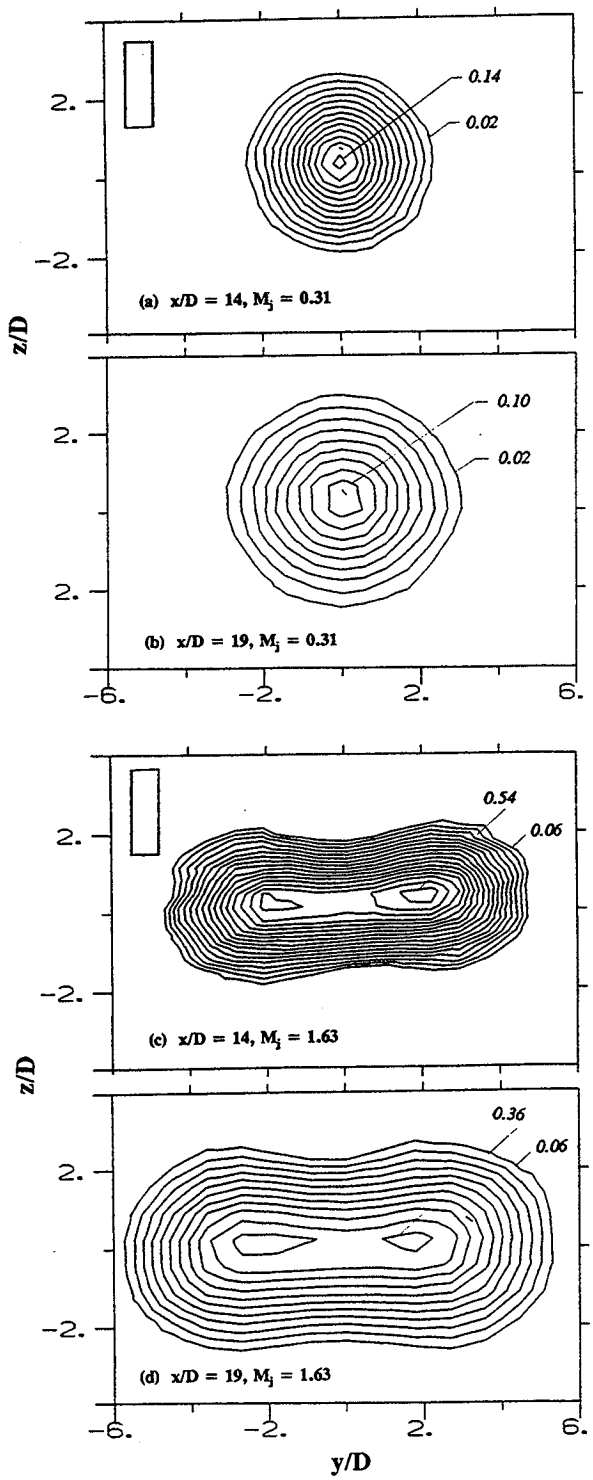

Figure 1 Mach number contours for a 3:1 rectangular jet (D = 1.47 cm) at indicated streamwise locations (x/D) and jet Mach numbers (M_j). The normalized mass flux (m/m_e, m_e being initial flux) for the four cases are: (a) 4.42, (b) 5.71, (c) 4.01, and (d) 5.40.

fact, the latter dynamics, referred to as the ω_X-*induced dynamics*, quite elegantly explain the effect of the tabs on the axis switching phenomenon. An objective of the present paper is to discuss the relevant results and elucidate these inferences.

It should be apparent that the ω_X- and the ω_θ-induced dynamics are not independent of each other. The distortion of the azimuthal vortex structures can lead to streamwise vortices even in the time averaged flow field, as demonstrated, for example, by the computational results of Ref. 17. Thus, the two dynamics interact and a resultant effect influences the evolution of the flow field. A set of experiments has been conducted in an attempt to shed light onto these interactions and the associated vorticity dynamics. Periodic forcing, via plenum chamber resonance, has been used to organize the azimuthal vortex structures. The method of phase averaging has been employed to investigate the vorticity field in unprecedented details for a specific case of the excitation. These experimental data illustrate such details of the flow field as the reorientation of the azimuthal vortex rings, their time variation, the nature and time variation of the streamwise vortex pairs, etc. These results are also discussed in this paper.

2. Experimental Method

The study was conducted with a 3:1 rectangular nozzle having an equivalent diameter, D = 6.35 cm. The essential features of the flow facility are shown schematically in Fig. 2. The nozzle contracted from a 41 cm round section to the 9.75cm x 3.25cm rectangular section within a length of 23 cm, the transition of the geometry starting at 12.7 cm from the exit. Compressed air was supplied through the other end of the plenum chamber and the flow discharged into the ambient. The plenum chamber had flow conditioning units, and the turbulence intensity at the jet exit center was approximately 0.15 percent. The nozzle exit boundary layer was measured at several peripheral locations. The momentum thickness over most of the two long edges was approximately $\theta/D = 0.004$. On the short edges and near the corners, deviations occurred by as much as 25 percent. From the shape factor the boundary layer was inferred to be nominally laminar everywhere.

Hot-wire measurements were carried out for a jet Mach number $M_j = 0.31$ which corresponded to a Reynolds number $Re_D \approx 450{,}000$. The flow field measurement technique was an extension of the method described in Ref. 2. Two X-wire probes, one in the u-v and the other in the

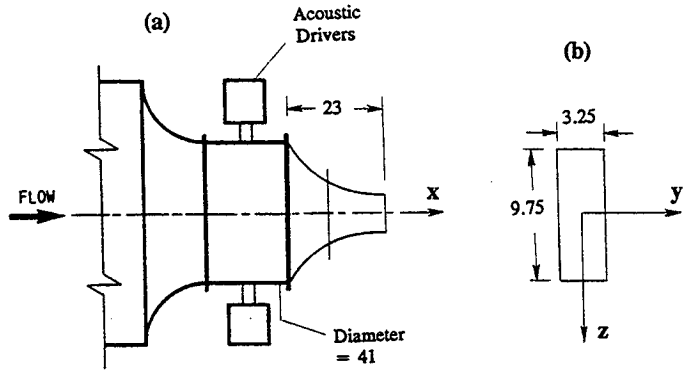

Figure 2 Schematic of jet facility; (a) side view of the exit section, (b) exit geometry of the rectangular nozzle. Dimensions are in cm.

u-w configuration, were traversed through the same grid points. The distributions of time averaged v and w in y and z yielded ω_X. Gradient correction was applied to all v and w data with a procedure similar to that used by Bell & Mehta.[18] For all data sets the hot-wires were calibrated at the start and the calibration was spot checked at the end of the run. When calibrating, the two X-probes were placed at the nozzle exit (tabs removed) centered around the axis. The CTA outputs from the four sensors were least-squares-fitted with fourth order polynomials as a function of the jet velocity. The polynomial coefficients were later used to calculate the velocities using cosine laws. The jet exit velocity (U_j) was measured from the plenum pressure which was constantly monitored during data acquisition. The data acquisition was stopped if U_j deviated more than $\pm 1.5\%$; data normalization was done by the updated value of U_j. The probe traverses and data acquisition were done by automated computer (Micro-Vax) control. The (Klinger) probe traverser had a resolution of 0.0025 cm.

The effect of the measurement grid size on the convergence of ω_X was tested. With the center of the grid coincident with the vortex center (determined by preliminary measurement), the grid size was progressively varied while measuring ω_X by line integration of v and w. Sufficiently small grid size was thus chosen for each x-station and used in the subsequent data acquisition. The uncertainty in the normalized streamwise velocity component within the core of the jet was estimated to be within $\pm 1\%$, and that in the

mean streamwise vorticity to be approximately ±20%; similar uncertainties were reported for past measurements.[19,20] However, progressively larger uncertainties and errors are expected away from the core. On the edges of the flow field especially, the hot-wire data are contaminated by occasional flow reversal. The data shown are as measured, and no correction is attempted. However, most of the vorticity data shown are within the higher speed regions of the jet and thus are thought to be free of such contamination.

The vortex generators used are the 'delta tabs'.[2] Each had a triangular shape with the base placed on the nozzle wall and the apex leaning downstream at an angle of 45°. The width of the tab at the base was 1.8 cm and the area blockage due to each was approximately 1.8 percent of the nozzle exit area.

An (Altec Lansing) acoustic driver was used for the excitation studies. The excitation was imparted in the form of 'plane wave' perturbation at the nozzle exit. The choice of the excitation frequency (f_p) was dictated by the plenum chamber resonances. Based on the studies of Ref. 8, which showed a large effect between Strouhal numbers (St = f_pD/U_j) of 0.45 and 0.85, a resonance at f_p = 1.01 kHz was chosen. This corresponded to St = 0.6; the maximum available amplitude of u'_{fe}/U_j = 0.004 was used, where u'_{fe} is the rms fundamental measured at the jet exit center.

The excitation signal was used as the reference for the phase averaging. A survey was conducted first and a subharmonic in the velocity spectra was noted to develop for x/D > 1.0. From the survey, x/D = 2.2 was chosen as the downstream limit for the measurements. Upstream of this station the subharmonic was deemed as minimal and not to affect the phase average process. From probe resolution considerations, on the other hand, the upstream limit for the measurements was set at x/D = 0.85. The time averaged data, however, were obtained over the range 0.5< x/D <20. The phase averaged data were acquired on-line for 19 phase points over a complete period of the fundamental. The convergence of the phase averaged data was tested initially, the data presented are typically averages over approximately 200 cycles. In the following the notation <f> is used to indicate phase average of a function f.

3. Results

3.1 Effect of tabs and excitation on axis switching:

Figure 3 shows the streamwise variations of the jet half-velocity-width measured on the major and the minor axis planes of the nozzle; B represents the distance between the points where the velocity is half of the local centerline velocity. One finds that within the x-range covered, the jet

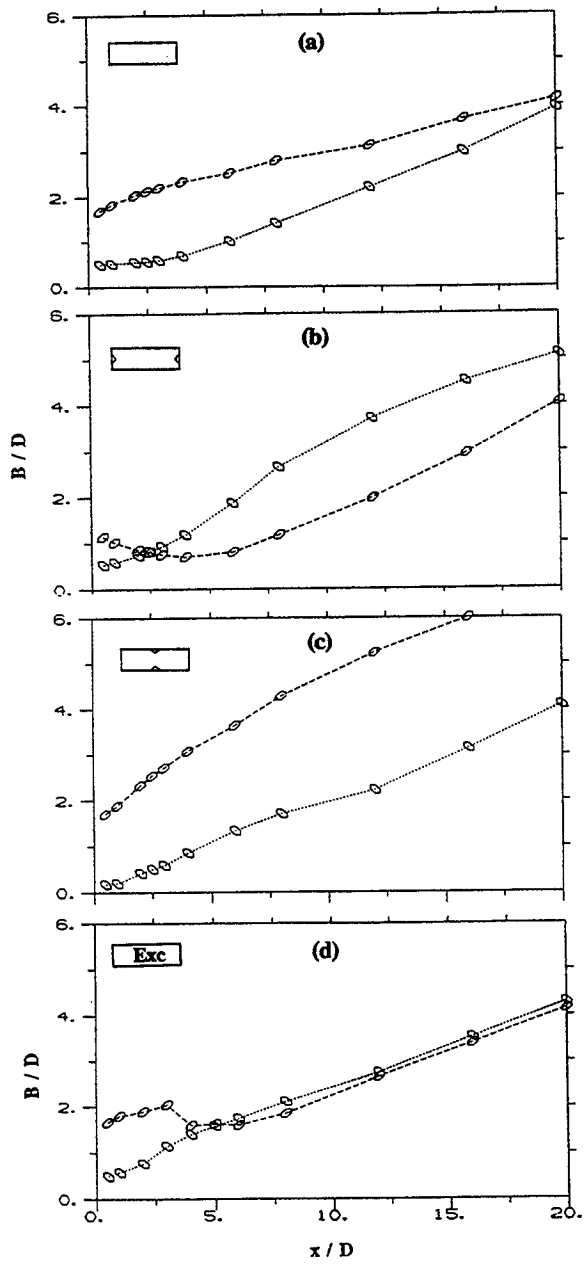

Figure 3 Streamwise variations of jet half-velocity-width; -o-, minor axis plane, -o-, major axis plane. (a) no tab, (b) two tabs on ends, (c) two tabs on sides, and (d) acoustic excitation at St = 0.6 and u'_{fe}/U_j = 0.004.

without any tabs has not gone through an axis switching (Fig. 3a). Two delta tabs placed on the narrow edges of the nozzle have caused a rapid switchover by x/D = 2.5 (Fig. 3b). In comparison, two delta tabs placed on the long edges have caused the jet to continue to diverge on the major axis plane within the measurement range (Fig. 3c). Figure 3(d) shows data obtained for the case of artificial excitation. Clearly, the excitation has also caused an early axis switching.

Data showing the time-averaged evolution of the flow fields corresponding to the four cases of Fig. 3(a)-(d) are presented in Fig. 4(a)-(d). Contours of longitudinal velocity are shown in the left column while the streamwise vorticity contours are shown in the right column, for the indicated x/D locations. Figure 4(a) shows that the undisturbed jet cross section has become essentially round by x/D = 16, and that the axes have not switched within this distance. Also, it is clear that streamwise vortices are present in this flow even without any tabs. One vortex originating from each corner of the nozzle dominates the flow field. The vortices are seen to lose their strength with increasing downstream distance and by x/D = 16 the amplitudes are below the measurement noise level.

Shortly downstream of the nozzle, the four vortices in the case of Fig. 4(a) form two counter-rotating pairs one on each end of the major axis. The sense of rotation, shown by the arrows with the data for x/D = 1, is such that there is an ejection of jet core fluid by each pair. That is, the fluid in between the two vortices of a pair is forced out into the ambient. For ease of identification such a vortex pair will be referred to in the following as the '*out-flow*' pair, and conversely, an '*in-flow*' pair will be of the opposite sense.

Here, it is instructive to examine similar time averaged vorticity results obtained by a few other investigators in comparable flows.[20-22] Quinn[20] reported data for a square nozzle. Pairs of counter-rotating streamwise vortices originated from each of the four corners of the nozzle. Thus, the flow field of the square jet was characterized by eight streamwise vortices instead of four seen in the rectangular case (Fig. 4a). Shortly downstream of the nozzle, two adjacent vortices on a side of the square cross section moved closer to each other to form an 'out-flow' pair. By x/D = 1.25 the two axes of the jet cross section interchanged position with the two diagonals, i.e., turned by 45°. Farther downstream, for x/D > 5, the jet cross section became practically round. The 45° switching of axes in a square jet will be addressed further in the following.

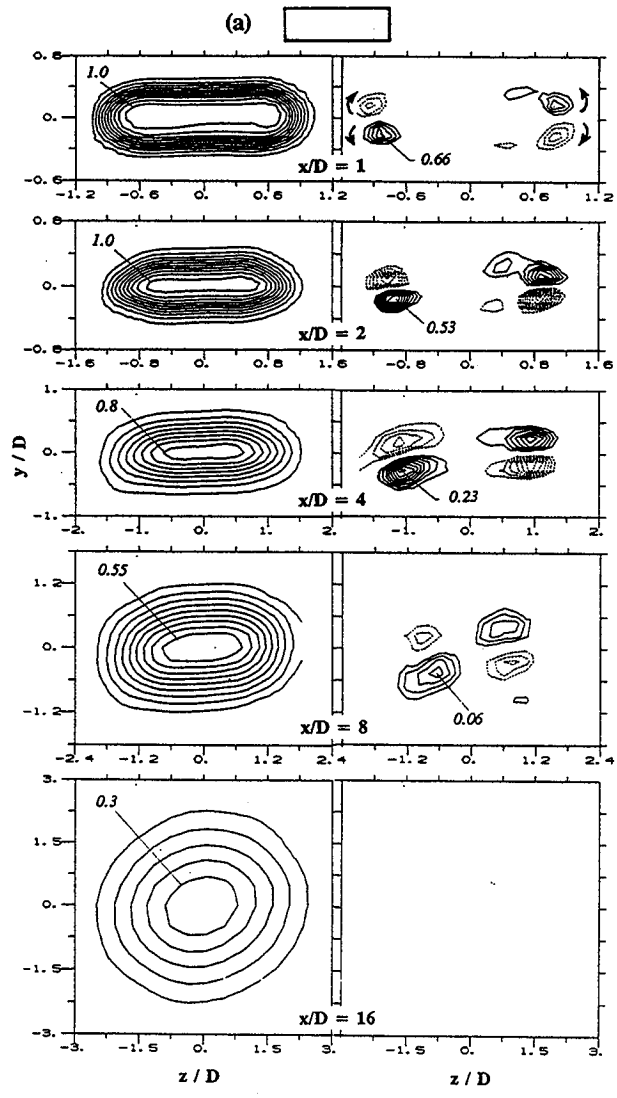

Figure 4(a)

Davis & Gessner[21] made measurements in a duct transitioning from circular to rectangular cross section. At the end of the rectangular section, their data showed the presence of four streamwise vortices. The distribution was quite similar to that measured in the present case, except that the sense of rotation was opposite, i.e., the two pairs formed at the ends of the major axis were of the 'in-flow' type. A subsequent computational study corroborated well with these experimental results.[23] The other experiment, of Miau *et al.*,[22] also involved a duct transitioning from circular to rectangular section of similar aspect ratio. There were only minor differences in the duct geometries. For example, the

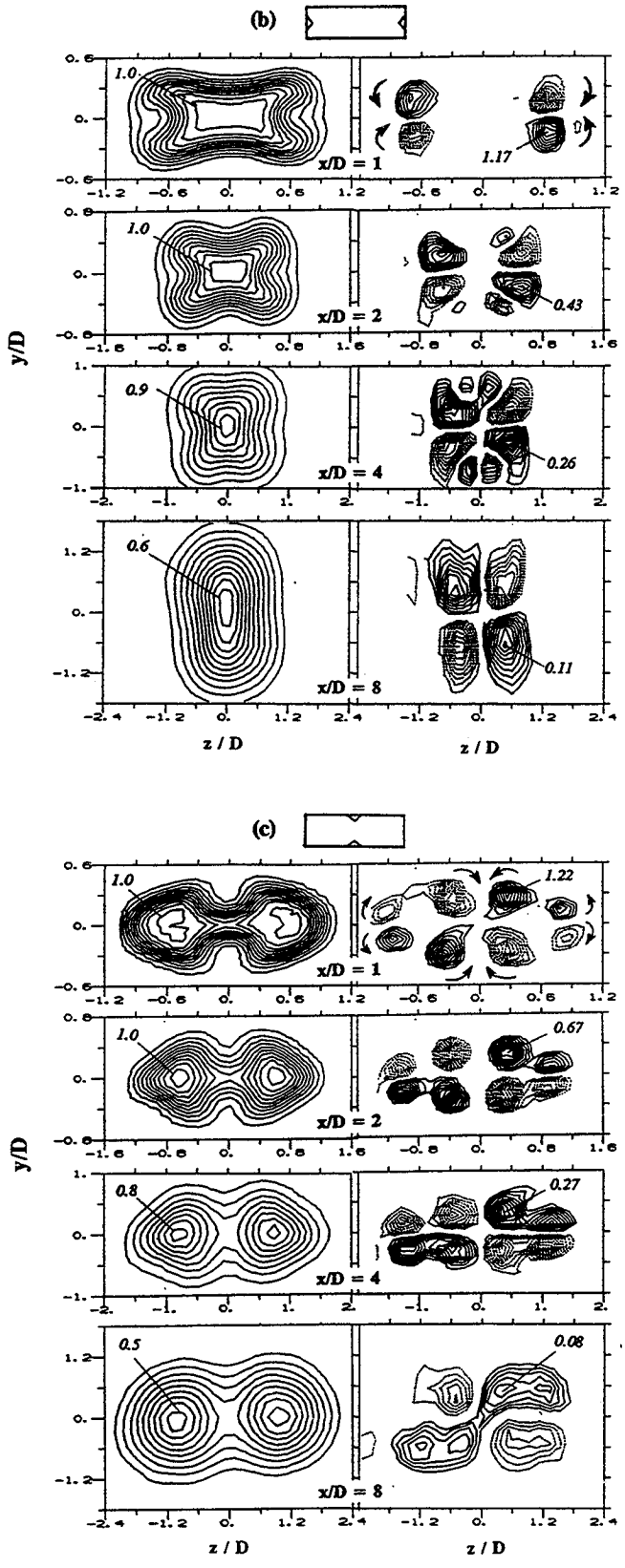

Figures 4(b),(c)

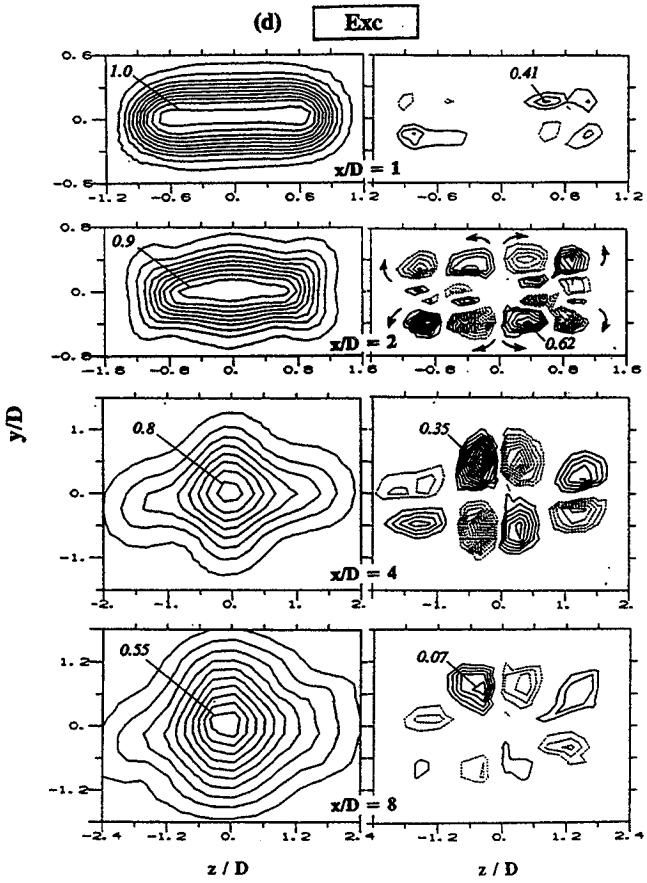

Figure 4 Contours of mean velocity (U/U_j, left column) and streamwise vorticity ($\omega_x D/U_j$, right column) for indicated x/D locations; (a)-(d) are for the corresponding tab and excitation cases of Fig. 3.

cross sectional area was held constant in the latter experiment while that in Davis & Gessner's[21] enlarged by 15% before reducing back to the inlet value. These differences, however, resulted in streamwise vorticity distribution in Miau *et al.*'s experiment with a sense opposite to that in Davis & Gessner's!

A primary source of streamwise vorticity in the flow through a transitioning duct is Prandtl's first kind of secondary flow, i.e., lateral pressure gradients skewing the boundary layer within the duct.[24] The flow is accelerated differently along different sections of the duct wall which gives rise to the lateral pressure gradients. While the experiments of Refs. 21 and 22 dealt with transitioning ducts with only minor variations in the cross sectional area, a jet nozzle involves large contraction ratios. For example, the con-

traction ratio with the present nozzle is over 40 (Fig. 2). As far as the sense of the streamwise vortices is concerned, it appears, from a consideration of the expected pressure gradients, that the 'out-flow' pairs should be the common ones in flows from convergent asymmetric nozzles. (Indeed, author's experiments with certain other asymmetric nozzles also yielded the 'out-flow' pairs.) Nevertheless, the contrast discussed in the preceding paragraph should make it amply clear that the geometry of the upstream flow path can have an impact on the distribution of the streamwise vortices occurring at the nozzle exit. Such a difference, in the initial ω_x-distribution, can have a profound influence on the subsequent evolution and axis switching of the free jet. This becomes evident from the data for the tab cases shown in Figs. 4(b) and 4(c).

Figure 4(b) shows data for the case with two delta tabs placed on the narrow edges. For space conservation data only up to x/D = 8 are shown for this and the subsequent cases. The tabs have generated two pairs of streamwise vortices which, as expected,[2] are of the 'in-flow' type. This is opposite to that occurring in the no tab case. The delta tabs have apparently overwhelmed the naturally occurring 'out-flow' pairs. However, two additional pairs of the latter sense are seen at x/D = 2 and 4. It is not clear, but these could be remnants of the naturally occurring vortices gathering strength because of the contraction of the flow in the direction of the major axis. The 'in-flow' vortex pairs produced by the tabs persist far downstream and the accompanying axis switching of the jet can be clearly seen from the mean velocity distributions.

When two delta tabs are placed on the long edges of the nozzle (Fig. 4c), two vortex pairs are introduced in addition to the naturally occurring vortices. Here, the proximity of like signed vortices induce amalgamation. The amalgamation is complete by x/D = 8, where the four pairs have yielded two pairs. The jet cross section in this case has not only stayed elongated in the major axis plane but has almost bifurcated. (Note that in all the cases of Fig. 4 a mild anti-clockwise turning of the jet cross section has taken place by the farthest downstream location. This, most likely due to a nonsymmetry in the recirculating flow within the laboratory, is also consistent with somewhat lower negative levels of ω_x compared to the corresponding positive levels observed at the downstream locations. However, this is inconsequential in the context of the present paper.)

The effect of the excitation on the evolution of the jet is shown in Fig. 4(d). A significant increase in the jet spreading can be observed from the mean velocity contours. This observation is in general agreement with that made in Refs. 7 and 8. Comparison of the data sets for x/D = 8 makes it apparent that the excitation (Fig. 4d) has increased the spreading more than that achieved by the two tab configurations (Figs. 4b and 4c). However, there are other tab and nozzle configurations which increase the spreading much more.[9] Note that the excitation results in a more complex ω_x distribution. Two additional pairs of vortices can be seen to emerge in the middle of the jet cross section which were absent closer to the nozzle exit. The additional streamwise vortices occurring farther downstream (x/D > 2) must trace their origin to the distortion and reorientation of the azimuthal vortex structures. This issue is addressed further in the following.

3.2 Mechanism of axis switching:

As stated before, Hussain & Husain,[8] while reporting their measurements for elliptic jets, provided an explanation for axis switching. This was based on the dynamics of the azimuthal vorticity. Figure 5 is a simplified version of one of their figures included here to help enunciate these *ω_θ-induced dynamics*. Consider a periodically forced elliptic jet, such as obtained by plane wave acoustic excitation. Shortly downstream of the nozzle the azimuthal vorticity rolls up into elliptic vortex rings. One such ring is

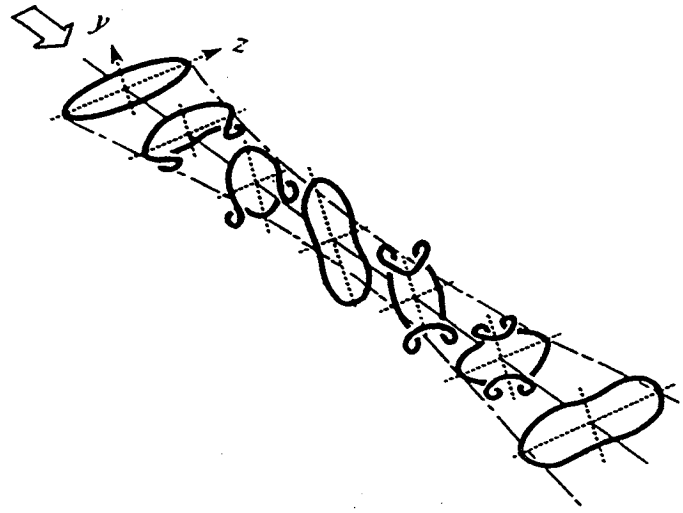

Figure 5 The 'ω_θ-induced dynamics'; sequence of deformations of an asymmetric vortex ring leading to axis switchings, from Hussain & Husain.[8]

represented by the structure on the left in Fig. 5. Due to difference in azimuthal curvature, a segment of the ring located at either end of the major axis has higher induced velocity compared to that of a segment located at either end of the minor axis. Thus, the former segment convects faster. Furthermore, the induced velocity of the segment is directed along its binormal (see the cited reference), thus, the faster moving segment also curls up and protrudes into the core of the jet. The initially elliptic ring, as a result, goes through a sequence of contortions. As represented by the fourth structure from the left, the ring approximately regains its original shape somewhere downstream except that the major and the minor axes are switched. The sequence of events can repeat farther downstream.

That such a process occurs with an isolated asymmetric vortex ring had been shown earlier.[13-15] Flow visualization pictures illustrating similar deformations of asymmetric vortex rings, in jets, have been shown in Refs. 7 and 8. In the forced jet, of course, this process occurs periodically. Successive vortex rings go through the same sequence of deformation. However, since the deformation of an individual ring is also a function of streamwise distance, the sequence shown in Fig. 5 reflects even on the time averaged flow field, and this leads to the axis switching of the jet.

While the description in the foregoing is given in terms of a periodically forced jet, the process also occurs in a natural asymmetric jet because there is natural roll up of the azimuthal vorticity. In the natural jet, however, the formation and subsequent evolution of the vortex rings are more random. The randomness results in a delayed axis switching or simply a transition to round shape without switching of the axes. Conversely, a periodic forcing of a natural jet organizes the coherent vortical structures which, by accentuating the ω_θ-induced dynamics, yields a faster axis switching. This is the effect seen in the data of Fig. 3(d) when compared to the data of Fig. 3(a). An earlier axis switching under the influence of acoustic excitation was also observed in Ref. 8 for an elliptic jet. This also explains why there had been an axis switching in the supersonic case of Fig. 1. The jet in that condition was screeching (at 6.3 kHz, further details in Ref. 9). An asymmetric jet with screech is also a periodically forced flow in which the faster axis switching is thought to have occurred by an accentuated ω_θ-induced dynamics.

The ω_θ-induced dynamics, however, do not clearly explain the observations made with the tabs. If it is assumed that the azimuthal vorticity rolls up with an initial shape similar to that determined by the downstream edges of the tabs and the nozzle, it might be possible to explain some of the observed trends. However, the flow fields are more complex for these cases, and the applicability of the ω_θ-induced dynamics is not straightforward. A much simpler and satisfactory explanation can be given in terms of the induced velocities of the streamwise vortex pairs. Consider the vortex pair, with equal and opposite strength $\pm\Gamma$ and spaced 2a, as sketched in Fig. 6(a). Recall from vortex dynamics that both the vortices will move to the right with a speed equal to $\Gamma/4\pi a$.[25] The fluid between them will also be ejected to the right at about four times this speed. Therefore, the dynamics of the two pairs of streamwise vortices sketched in Fig. 6(b), representative of the natural jet case (Fig. 4a), would tend to elongate the jet cross section in the direction of the major axis. Conversely, for the distribution sketched in Fig. 6(c), representative of the

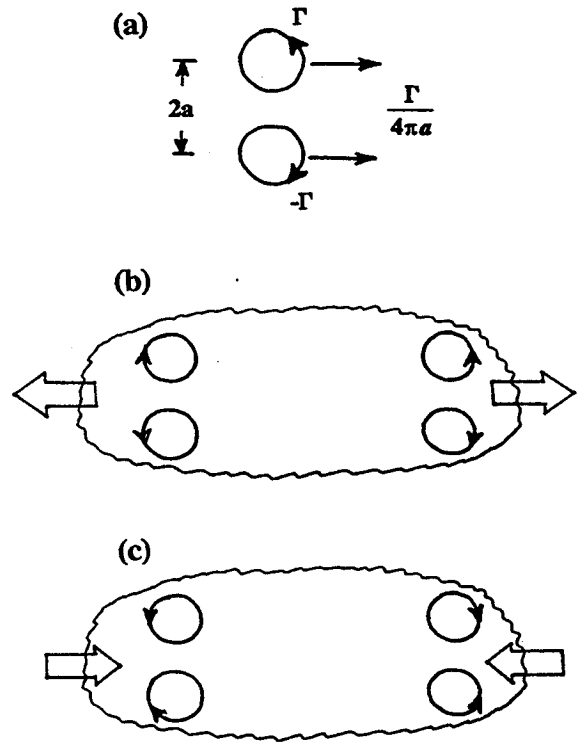

Figure 6 The 'ω_x-induced dynamics'; (a) induced velocities of a vortex pair, (b) distribution of streamwise vortex pairs resisting axis switching, (c) distribution promoting axis switching.

tab case of Fig. 4(b), both pairs would move towards the jet centerline. This would result in a contraction of the jet cross section in the direction of the major axis.

It should follow, therefore, that the ω_x-induced dynamics described in the foregoing would resist axis switching in the natural jet case of Fig. 4(a). On the other hand, axis switching would be promoted in the tab case of Fig. 4(b). These are indeed the observed trends. Note that in the cases of Figs. 4(b) and 6(c), once the two pairs of vortices have moved close to each other the new pairs formed above and below the major axis would then move away from the jet axis. The vortex distribution in this case, therefore, supports an efficient mechanism causing the *first* axis switchover. It should be clear that the ω_x-induced dynamics will not support further axis switchings beyond the first. Possible further switchings may occur only through the ω_θ-induced dynamics. It should also be easy to see that the induced velocities of the vortex pairs in the case of Fig. 4(c) are similar to that in the natural jet case (Fig. 4a), i.e., all four pairs move away from the jet centerline in the direction of the major axis. The jet cross section thus elongates in that direction. In fact, due to the additional vortices, the pull is so much that the jet cross section is essentially bifurcated.

The ω_x-induced dynamics can also explain the 45° axis switching observed in the square jet experiment of Quinn.[20] Quinn's measurements showed four 'in-flow' pairs of vortices occurring close to the nozzle exit at x/D = 0.28, as sketched in Fig. 7(a). It is not completely clear, but the origin of these vortices is also thought to be upstream secondary flow as in Davis & Gessner's experiment.[21] With the given vorticity distribution, in any case, it should be easy to see that each vortex pair at first moves towards the jet centerline. Two vortices on a side then form an 'out-flow' pair. The four resulting pairs then move away from the jet centerline, as sketched in Fig. 7(b), causing the 45° switching of the axes.

A similar 45° axis switching has also been observed with a periodically forced square jet in the computational study of Grinstein.[26] In the computation, however, there is no streamwise vorticity initially. Thus, the 45° switching in that flow must have occurred due to the dynamics of the azimuthal vorticity. The azimuthal vorticity initially rolls up into a square ring. The corners of the ring then deform and reorient in a manner similar to that described with Fig. 5, and this eventually results in the 45° axis switching. The "volume visualization" of vorticity presented by Grinstein provides an insight into these processes (see also Ref. 17).

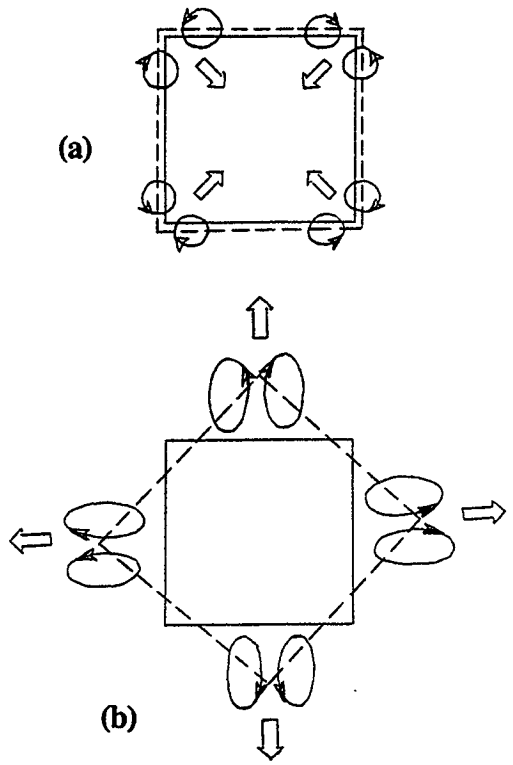

Figure 7 Schematic of mean streamwise vorticity distributions in a square jet, after the results of Quinn (1992); (a) distribution close to the jet exit, (b) distribution farther downstream.

The axis switchings observed by Toyoda *et al.*,[11] with orifice jets of various cross sections, apparently also occurred due to the ω_θ-induced dynamics.

It is likely that a combination of the ω_θ- and ω_x-induced dynamics may also explain the difference in the behavior of jets from "slot nozzles" with and without an upstream contraction.[10] In the case without the contraction, most likely the former dynamics played the dominant role to cause the axis switching. With the upstream contraction the flow field could be similar to that in the present natural jet (no tab, no excitation case, Fig. 4a). The likely presence of 'out-flow' vortex pairs could have, similarly as in the present case, resisted the axis switching.

It should be quite apparent by now that the ω_θ- and ω_x-induced dynamics may not be independent of each other. The streamwise vortices are embedded in a sheet of azimuthal vorticity. Thus, the ω_x- dynamics are influenced by the forces exerted by the latter vorticity field. Conversely, the reorientation of the azimuthal vorticity gives rise to streamwise vortex pairs the influence of which constitutes an

integral part of the ω_θ-induced dynamics. The following experiment was conducted in an effort to gain further insight into these complex processes.

3.3 Phase averaged vorticity field for the excitation case:

Corresponding to the excited case of Figs. 3(d) and 4(d), detailed phase averaged flow field measurements were carried out. The underlying concepts and the procedure were the same as in Ref. 19. The excitation signal was used as reference. The same probe arrangement as described in §2 was used. The four hot-wire signals and the reference signal were sampled simultaneously. The phase averaging was performed on-line using the peaks in the reference signal as triggers. The $<u>$, $<v>$ and $<w>$ data for 19 phases, within a period, were stored for each of the grid points on a y-z plane. As done with the time averaged data, gradient correction for $<v>$ and $<w>$ were performed based on the $<u>$ gradients. These data were post processed to obtain streamwise vorticity, $<\omega_X> = \partial<w>/\partial y - \partial<v>/\partial z$. The terms $<\omega_Y>$ and $<\omega_Z>$ were calculated invoking the Taylor hypothesis as, $<\omega_Y> = \partial<u>/\partial z + (1/U_c)\partial<w>/\partial t$, and $<\omega_Z> = -(1/U_c)\partial<v>/\partial t - \partial<u>/\partial y$. Here, the notation t represents time with respect to a trigger location, and U_c is a convection velocity assumed to be $0.5U_j$.[27] From the two azimuthal components of vorticity the quantity, $<\xi> = (<\omega_Y>^2 + <\omega_Z>^2)^{1/2}$ was calculated which closely approximated enstrophy. Its significance is described further in the following. The distributions of $<\omega_X>(y,z,t)$ and $<\xi>(y,z,t)$ were obtained at a number of streamwise locations. From these data spatial distributions of these properties could be constructed over a volume of the flow field for a given phase.

The distributions of $<\omega_X>$, on a cross sectional plane of the jet at x/D = 2, are shown in Fig. 8 for four phases (ϕ), as examples. The phases are chosen approximately at equal intervals within the period. Note that the time averaged ω_X distribution corresponding to these data were shown in Fig. 4(d). The data in Fig. 8 show that the streamwise vorticity distribution goes through dramatic changes with time (i.e., phase) within a period. Compare, for example, the data for $\phi = 0°$ and 176°. The dominant vortex pairs in the two plots are of opposite sense! These data underscore the fact that the vorticity dynamics is much more vigorous than what is revealed by the time averaged flow field. In a flow downstream of a 'delta tab' Bohl & Foss[28] have measured the r.m.s. of ω_X to be as much as six

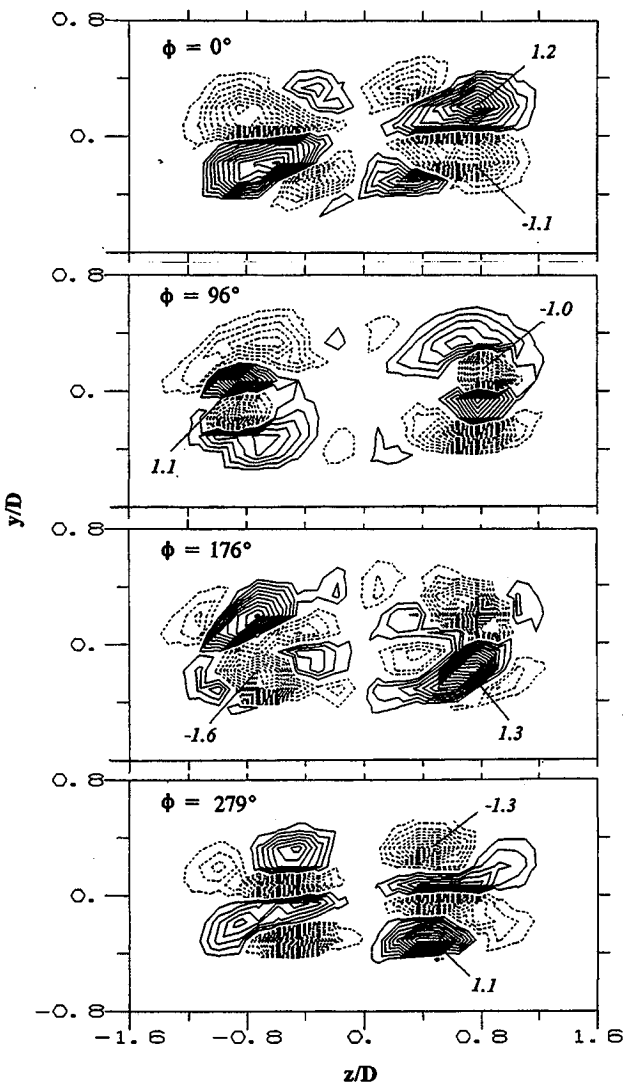

Figure 8 Contours of phase averaged streamwise vorticity, $<\omega_X>D/U_j$, measured at x/D = 2 for the excitation case. The four sets of data are for indicated phases (ϕ).

times larger than the corresponding mean amplitude. In the present flow, the time averaged ω_X near the jet exit is of small magnitude (x/D = 1, Fig. 4d), but the amplitudes are seen to actually increase farther downstream. The appearance of larger amplitude ω_X farther downstream, as well as the reversals in the $<\omega_X>$ distributions in Fig. 8, can be traced to a reorientation of the azimuthal vorticity. This becomes clear with the following data.

Figure 9 shows the time variation of an iso-surface of $<\xi>$, on the y-z plane at x/D =2. The variation includes all 19 phase points approximately covering the full

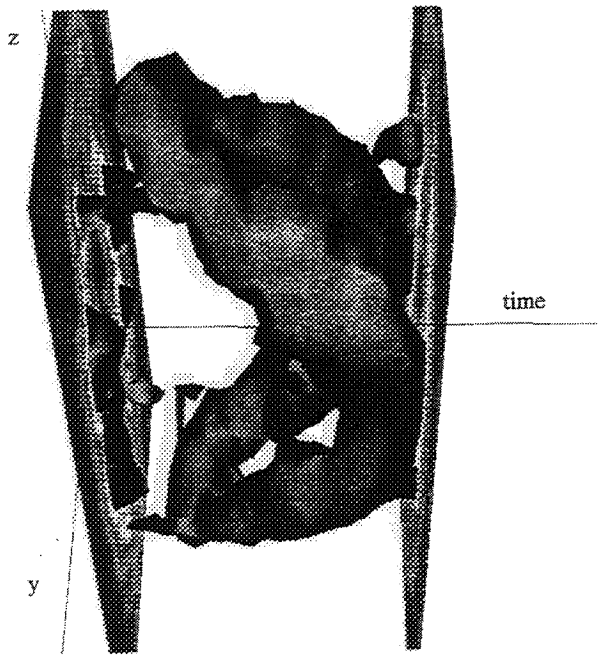

Figure 9 Temporal distribution of an iso-surface of enstrophy, $<\xi>D/U_j = 2.7$, measured at x/D = 2.0, shown over a complete period of the excitation.

period. Since the magnitude of either $<\omega_Y>$ or $<\omega_Z>$ is significantly larger than that of $<\omega_X>$, $<\xi>$ closely approximates enstrophy the true value of which would also include contribution from $<\omega_X>$. With an appropriate choice of the iso-surface level, $<\xi>$ provides an indication of the concentration of the azimuthal vorticity within the flow field. Inspection of Fig. 9 reveals the presence of a distorted vortex ring. The azimuthal vorticity which initially rolls up into an approximately elliptic shaped vortex ring has gone through a contortion by x/D = 2, in a manner similar to that described with Fig. 5. Note that positive time corresponds to negative x, and thus, the distortion appears reverse. To the author's knowledge, this is a first set of *experimental data* quantitatively confirming such distortion seen earlier mainly by flow visualization.[7,8]

The spatial distributions of $<\xi>$ over the full volume of the flow field are shown in Fig. 10. While Fig. 9 showed temporal distribution at a fixed x/D, each set of data in Fig. 10 represents spatial distribution for a fixed phase. The four data sets correspond to the same four phases of Fig. 8. For display purposes the x-coordinate has been stretched by a factor of 2 and the origin is shown at x/D =

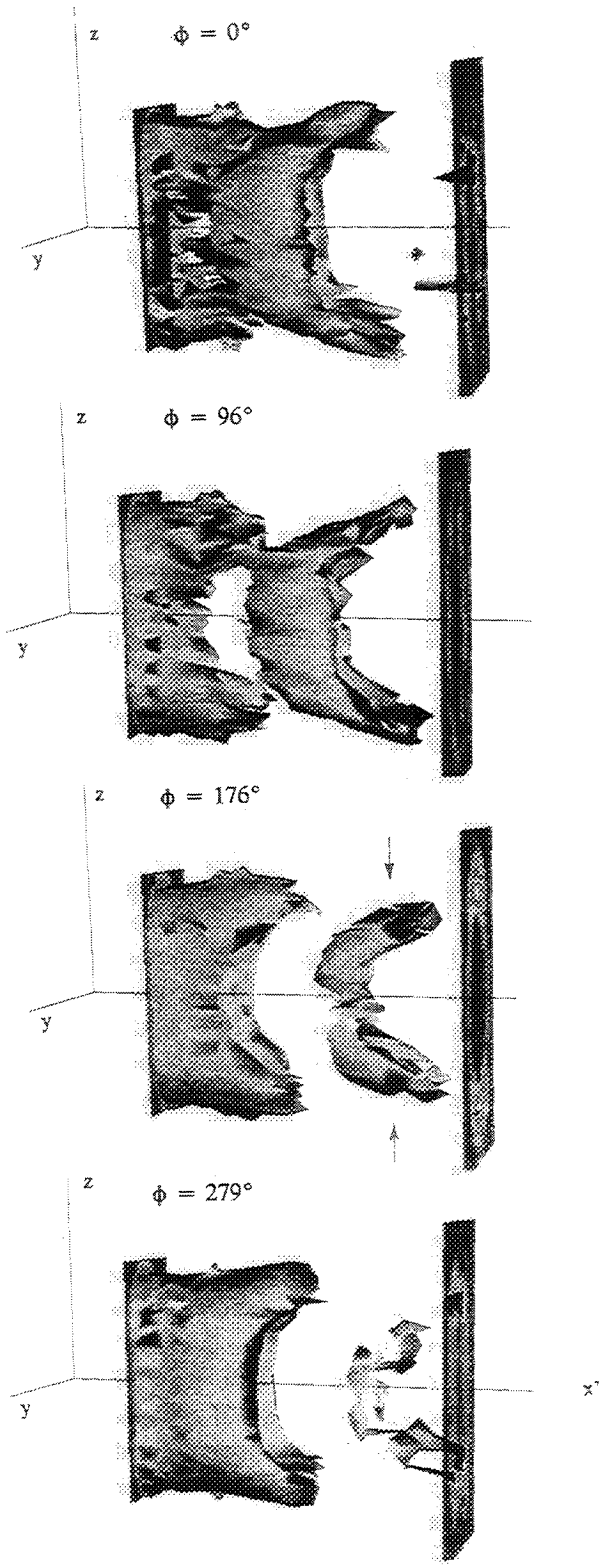

Figure 10 Spatial distributions of an iso-surface of enstrophy, $<\xi>D/U_j = 3.2$, for the four phases of Fig. 8.

0.5 instead of at x/D = 0; i.e., x' = (x - 0.5D)*2. The data covers the region from x/D = 0.85 to 2.2. Also, since the magnitude of $<\xi>$ decreases substantially with increasing x, the choice of a level for the iso-surface enabling a visualization of the whole flow field was difficult. A small level would mask the details of the coherent structures while a large level would show them only at the upstream locations. The level indicated in the figure caption was chosen after some trial.

The evolution of the azimuthal vorticity field with time is captured by the data in Fig. 10. The sheet of azimuthal vorticity emerging from the nozzle can be seen to form isolated structures. Such a structure is about to break off in the data set for $\phi = 0°$. The segments at the ends of the major axis are already tilted forward. These apparently become more tilted as the structure propagates downstream. It should be apparent that such deformations contribute to the x-component of vorticity which is further illustrated in the following.

The temporal distributions of $<\omega_x>$ corresponding to the data of Fig. 9 are shown in Fig. 11. Two views, approximately projecting on the major and the minor axis planes, are shown. Since $<\omega_x>$ involves negative and positive amplitudes, two iso-surfaces are required to show these variations. The data provide a comprehensive picture of the $<\omega_x>$ field. At a given instant the y-z plane contains two streamwise vortex pairs. These two pairs are of a certain sense ('in-flow' or 'out-flow'). Approximately one half period away, as was seen in Fig. 8, the same y-z plane contains two pairs with an opposite sense.

A clearer idea about the sense of rotation of the streamwise vortex pairs is obtained from the spatial distributions of $<\omega_x>$. Such distributions, corresponding to the four phases of Fig. 10, are shown in Fig. 12. Clearly, the flow field at a given phase is characterized by two pairs of streamwise vortices which alternate in sense with varying x. Now let us consider the two vortex pairs marked by the vertical arrows in the data set for $\phi = 176°$. The same locations in the corresponding data set of Fig. 10 are also marked by two vertical arrows. If the isolated vortex structure in Fig. 10 at this location is considered, it should not be difficult to see that the tilting of the narrow ends of the structure must generate two 'in-flow' pairs of streamwise vortices. These are the two pairs seen in Fig. 12 at the corresponding arrow locations. The two preceding vortex pairs in Fig. 12, marked by the inclined arrows, have the 'out-flow' sense of rotation. The deformation of an azimu

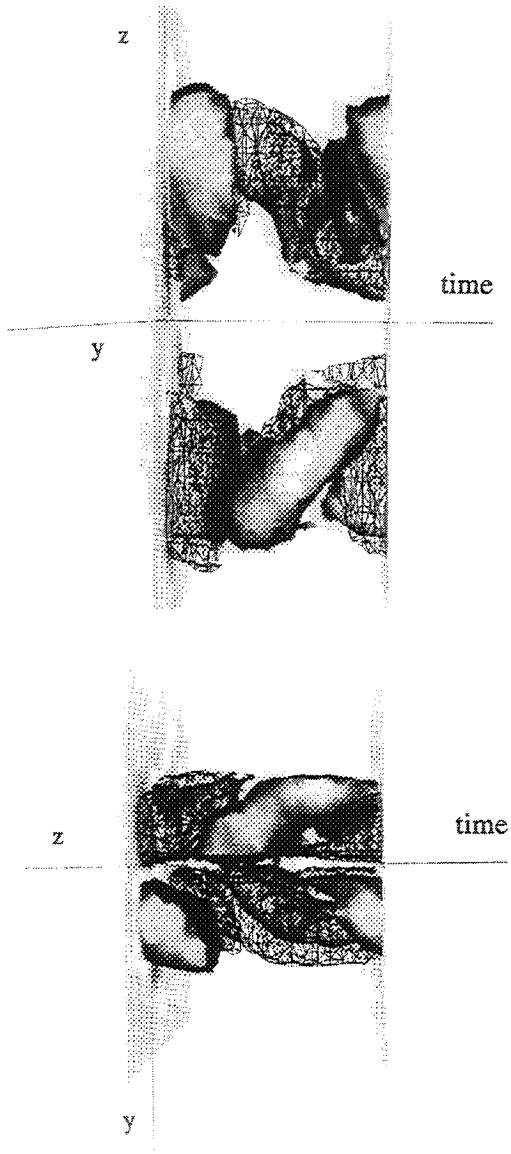

Figure 11 Temporal distributions of two iso-surfaces of streamwise vorticity, $<\omega_x>D/U_j = 0.3$ (solid) and -0.3 (transparent net-like), measured at x/D = 2. The two images are two views of the same set of data.

thal vortex ring, as seen in Figs. 10 and 11, however, *can not* produce streamwise vortex pairs with this sense. Then where are these arising from?

The answer most likely traces to another feature of the vorticity field that has not been addressed so far. Referring back to Fig. 4, one might ask as to how were the streamwise vortices originating from secondary flow within

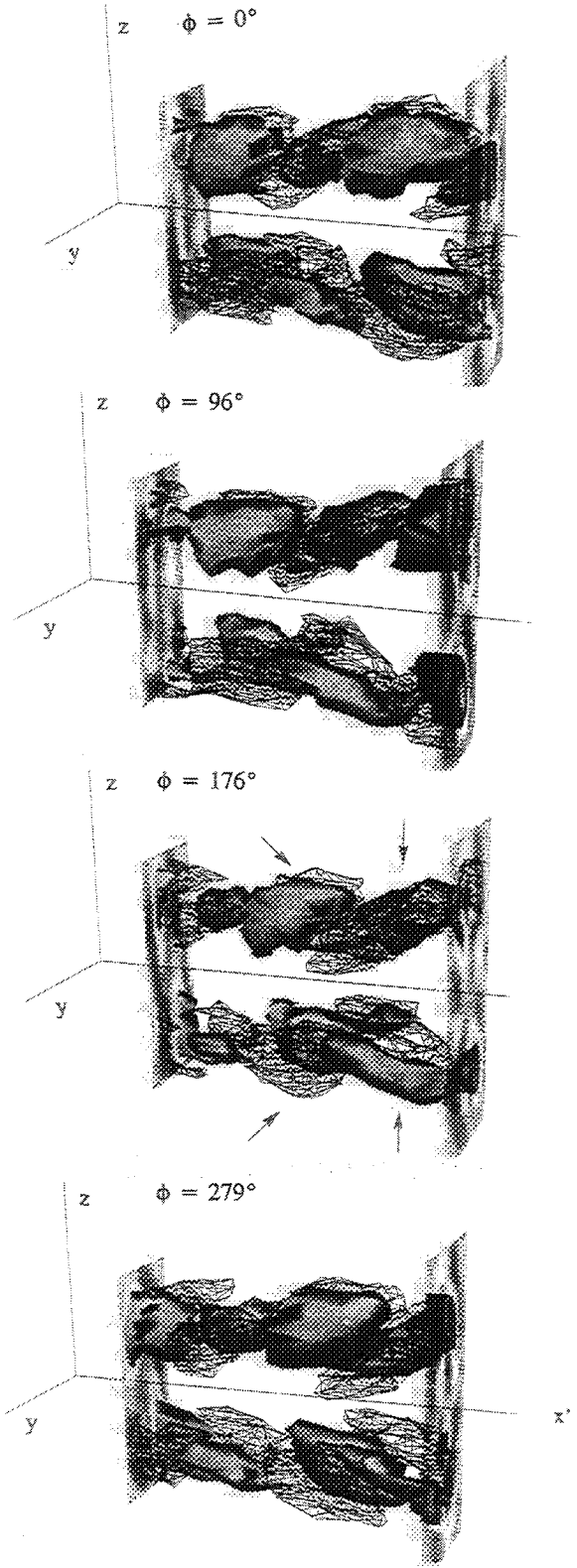

Figure 12 Spatial distributions of iso-surfaces of streamwise vorticity, $<\omega_x>D/U_j = \pm 0.3$, for the four phases of Figs. 9 and 11.

the nozzle (seen in (a)) affected by the periodic excitation (in (d)). It is unlikely that the excitation has appreciably changed the flow field within the nozzle. Excitation, with comparable amplitudes, has been known not to alter even the boundary layer state at the nozzle exit.[29] The source of the streamwise vortices (Prandl's first kind of secondary flow) must, therefore, be present even under the excitation. It is apparent that the 'out-flow' pairs of vortices originating from this source have been redistributed by the excitation. The excitation has lumped this vorticity periodically in space. It is thought that this is how the vortex pairs marked by the inclined arrows in Fig. 12 have appeared. Thus, on either side of the minor axis plane, an 'in-flow' pair generated by the reorientation of ω_θ is followed by an 'out-flow' pair that traces its origin to secondary flow within the nozzle. The sequence is repeated with the passage of each vortical structure.

Finally, Fig. 13 shows the distribution of time averaged ω_x over the measurement volume. This distribution may be compared with the phase averaged data of Fig. 12. It should be apparent from the choice of the iso-surface levels that the time averaged amplitudes, as expected, are much smaller than the corresponding phase averaged amplitudes. The time averaged streamwise vortices have resulted from a combination of contributions from the nozzle secondary flow and the distortion of azimuthal vorticity. The distribution is complex, as was also indicated by the data of Fig. 4(d), and involves several vortex pairs. Towards the

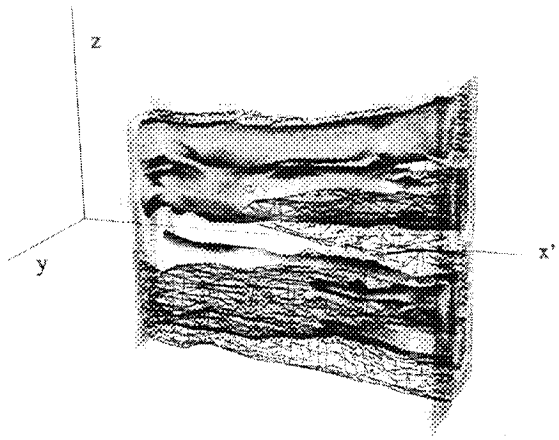

Figure 13 Spatial distribution of time averaged streamwise vorticity, $\omega_x D/U_j = \pm 0.11$.

downstream end of the measurement volume four pairs of vortices can be identified. The outer two pairs are of the 'out-flow' sense and must be mainly due to the nozzle secondary flow. The inner two pairs, of the 'in-flow' sense, must be mainly due to the deformation of the azimuthal vortex rings. It is remarkable that out of the vigorous time-dependent activity these distinct vortex pairs emerge in the time averaged flow field. The ω_X-induced dynamics associated with the four pairs are also consistent with the characteristic deformation of the jet cross section observed at the downstream locations of Fig. 4(d).

Concluding Remarks:

In this paper the results of an experimental study on a free rectangular jet have been presented. Vortex generators in the form of tabs are used to introduce streamwise vortices and periodic excitation is used to organize the azimuthal coherent structures. Both of these affect the phenomenon of axis switching and thus provide insight into the underlying mechanisms.

The basic flow, without excitation or vortex generators, is characterized by four streamwise vortices which trace their origin to secondary flow within the nozzle. These form two counter-rotating pairs each located on either end of the major axis. These are of the 'out-flow' type, i.e., with a sense of rotation so as to eject jet core fluid into the ambient. These vortices fade away by x/D = 16, and the jet does not go through an axis switching by that distance. The use of two delta tabs, placed on the narrow edges of the nozzle, cause changes in the flow upstream to produce two opposite, 'in-flow' pairs. The jet in this case goes through a rapid axis switching. Two delta tabs placed on the long edges of the nozzle, on the other hand, produce vortex pairs with sense similar to those existing in the natural case. The like signed vortices amalgamate and the jet continues to diverge on the major axis plane within the measurement range.

Two mechanisms are identified for the axis switching. One, addressed previously by others, is due to the deformation and reorientation of rolled up azimuthal vortices. This mechanism, referred to as the ω_θ-induced dynamics, always tends to cause axis switching. As the azimuthal coherent structures evolve and persist in the flow, it continues to act causing a second or even a third axis switching. However, randomness dilutes the effect and the latter switchovers are usually not clearly detectable. Randomness also affects the first switchover and causes its location to shift downstream. Conversely, when a jet is forced periodically, which organizes the azimuthal coherent structures and removes some of the randomness, it causes the first switchover to occur farther upstream. This has been readily demonstrated in previous, and in the present, experiments by periodic excitation. This is also thought to be the mechanism causing a faster axis switching in screeching supersonic jets, as screech is also a periodic excitation which accentuates the ω_θ-induced dynamics.

The second mechanism, identified in this study and referred to as the ω_X-induced dynamics, is due to induced velocities of streamwise vortex pairs. Two pairs of streamwise vortices, situated at the ends of the major axis and having the 'out flow' sense, resist axis switching. Such vortex pairs are often present in jets due to secondary flow within the nozzle, especially when the nozzle involves round-to-asymmetric contraction sections. Thus, in such jets axis switching is either delayed or may not occur. On the other hand, if two 'in-flow' vortex pairs are situated at the ends of the major axis the effects of the ω_θ- and the ω_X-induced dynamics supplement each other and cause a rapid axis switching. This was the case when two tabs were located on the narrow edges of the nozzle. Conversely, when two tabs were located on the long edges, the 'out-flow' vortex pairs were reinforced to provide additional resistance to axis switching.

Thus, cancelling effects between the ω_θ- and ω_X-induced dynamics are thought to be responsible for a slow or no axis switching occuring with many asymmetric nozzles. With asymmetric orifices, on the other hand, a rapid axis switching is due to the dominance of the ω_θ-induced dynamics. Since there is no significant upstream secondary flow to produce streamwise vortices the opposing effect of ω_X-induced dynamics is absent in this case. Either of the ω_X- or ω_θ-induced dynamics can also explain a 45° axis switching observed with square jets.

The two dynamics are obviously not independent of each other. The streamwise vortices are embedded in a sheet of azimuthal vorticity. Thus, the forces exerted by the latter vorticity field affect the ω_X-induced dynamics. On the other hand, the reorientation of the azimuthal vorticity generates streamwise vortex pairs. The forces exerted by such vortex pairs become integral part of the ω_θ-induced dynamics. In fact, the observed reorientation of an azimuthal vortex produces streamwise vortex pairs with the 'in-flow' sense. These vortex pairs augment the effect of the ω_θ-induced dynamics contributing to a faster axis switching.

For a periodically forced jet, a detailed set of phase averaged data are presented in this paper. For a volume of the near flow field, the data show the distribution of the streamwise vortices as well as the azimuthal vortical structures. Data for different phases capture the time variation of these structures. The reorientation of an azimuthal vortex structure, erstwhile seen in flow visualization and computational studies, is demonstrated by these data.

The periodic excitation is observed to alter even the time averaged streamwise vorticity distribution. At about two equivalent diameters downstream, while the natural flow contains only two 'out-flow' pairs, the excitation results in four pairs. An examination determines that the outer two of these four pairs trace to the nozzle secondary flow while the inner two originate from the reorientation of the azimuthal vorticity. The 'out-flow' streamwise vortex pairs, due to secondary flow within the nozzle, become redistributed by the excitation. These vortex pairs become periodically lumped in space, with the intervening regions containing vortex pairs of opposite sense occurring from the reorientation of azimuthal vorticity. Thus, the time variation at a given location exhibit vortex pairs of alternating sense. The phase averaged flow field, therefore, is characterized by much more vigorous vortical activity than that revealed by the time averaged flow field.

Acknowledgement: The author is grateful to Dr. Judith K. Foss for a careful review of the manuscript.

References:

[1]Ahuja K. K. and Brown W. H., 1989, "Shear flow control by mechanical tabs", *AIAA Paper* No. 89-0994.

[2]Zaman K.B.M.Q., Reeder M.F., and Samimy M., 1994, "Control of an axisymmetric jet using vortex generators", *Physics of Fluids A, 6* (2), pp. 778-793.

[3]Sforza, M.P., Steiger, H.M. and Trentacoste, N., 1966, "Studies on three-dimensional viscous jets", *AIAA J., 4*, pp. 800-806.

[4]Sfeir, A.A., 1976, "Investigation of three-dimensional turbulent rectangular jets", *AIAA Paper* 78-1185.

[5]Krothapalli, A., Baganoff, D. and Karamcheti, K., 1981, "On the mixing of rectangular jet", *J. Fluid Mech., 107*, p.201.

[6]Tsuchiya, Y., Horikoshi, C. and Sato, T., 1986, "On the spread of reactangular jets", *Experiments in Fluids, 4*, p. 197.

[7]Ho, C.-M. and Gutmark, E., 1987, "Vortex induction and mass entrainment in a small-aspect-ratio elliptic jet", *J. Fluid Mech.*, vol. 179, pp. 383-405.

[8]Hussain F. and Husain H.S., 1989, "Elliptic jets. Part 1. Characteristics of unexcited and excited jets", *J. Fluid Mech.*, 208, pp. 257-320.

[9]Zaman K.B.M.Q., 1994, "Effect of 'delta tabs' on mixing and axis switching in jets from asymmetric nozzles" *AIAA Paper* 94-0186, Aerospace Sciences Meeting, Reno, NV, Jan.

[10] Gutmark, E. and Schadow, K.C., "Azimuthal instabilities and mixing characteristics of a small aspect ratio slot jet", *AIAA Aerospace Sciences Meeting (87-0486)*, Reno, NV, Jan. 1987.

[11]Toyoda, K., Shirahama, Y. and Kotani, K., 1991, "Manipulation of vortical structures in noncircular jets", *ASME Forum on Turbulent Flows, FED 112*, Book No. G00600, pp. 125-140.

[12]Hertzberg, J.R. & Ho, C.-M., 1992, "Time-averaged, three-dimensional flow in a rectangular sudden expansion", *AIAA J., 30*(10), pp. 2420-2425.

[13]Kambe, T. & Takao, T., 1971, "Motion of distorted vortex rings", *J. Phys. Soc. Japan, 31*(2), pp. 591-599.

[14]Viets, H. and Sforza, P.M., 1972, "Dynamics of bilaterally symmetric vortex rings", *Physics of Fluids, 15*(2), pp. 230-240.

[15]Dhanak, M.R. and Bernardinis, B.D., 1981, "The evolution of an elliptic vortex ring", *J. Fluid Mech., 109*, pp. 189-216.

[16]Kiya, M., Ishii, H. and Kitamura, M., 1991, "Simulating deformation of non-circular vortex rings", *ASME Forum on Turbulent Flows, FED 112*, Book No. G00600, pp. 115-120.

[17]Grinstein, F.F., Gutmark, E, and Parr, T., 1994, "Numerical and experimental study of the near field of subsonic, free square jets", AIAA Paper 94-0660, Aerospace Sciences Meet., Reno, NV, Jan.

[18]Bell J.H. and Mehta R.D., 1992, "Measurements of the streamwise vortical structures in a plane mixing layer", *J. Fluid Mech., 239*, p. 213.

[19]Hussain, A.K.M.F. and Zaman, K.B.M.Q., 1980, "Vortex Pairing in a Circular Jet under Controlled Excitation. Part 2. Coherent Structure Dynamics", *J. Fluid Mech., 101*, pp. 493-544.

[20]Quinn, W.R., 1992, "Streamwise evolution of a square jet cross section", *AIAA J., 30*(12), Dec.

[21]Davis, D.O. and Gessner, F.B., 1992, "Experimental investigation of turbulent flow through a circular-to-rectangular transition duct", *AIAA J., 30*, p. 367, Feb.
[22]Miau, J.J., Leu, T.S., Chou, J.H., Lin, S.A. and Lin, C.K., 1990, "Flow distortion in a circular-to-rectangular transition duct", *AIAA J., 28*, p.1447.
[23]Sotiropoulos, F. and Patel, V.C., 1993, "Numerical calculation of turbulent flow through a circular-to-rectangular transition duct using advanced turbulence closures", *AIAA 93-3030*, Fluid Dynamics Conf., Orlando, FL, July.
[24]Bradshaw, P., 1987, "Turbulent secondary flows", *Ann. Rev. Fluid Mech., 19*, p. 53.
[25]Eskinazi, S., 1967, "Vector mechanics of fluids and magnetofluids", *Academic Press*, New York.
[26]Grinstein, F.F., 1993, "Vorticity dynamics in spatially-developing rectangular jets", *AIAA Paper* 93-3286, Shear Flow Conference, Orlando, FL, July.
[27]Zaman, K.B.M.Q., Hussain, A.K.M.F., 1981, "Taylor Hypothesis and Large-scale Coherent Structures", *J. Fluid Mech., 112*, pp. 379-396.
[28]Bohl, D.G. and Foss, J.F., 1994, "Streamwise vorticity and velocity measurements in the near field of a tabbed jet", *ASME* Meeting, Chicago, IL, June.
[29]Zaman K.B.M.Q. and Hussain A.K.M.F., 1980, "Vortex Pairing in a Circular Jet under Controlled Excitation. Part 1. General Jet Response", *J. Fluid Mech., 101*, pp. 449-491.

REPORT DOCUMENTATION PAGE

Form Approved
OMB No. 0704-0188

1. AGENCY USE ONLY (*Leave blank*)	2. REPORT DATE	3. REPORT TYPE AND DATES COVERED
	November 1994	Technical Memorandum

4. TITLE AND SUBTITLE

Axis Switching and Spreading of an Asymmetric Jet—Role of Vorticity Dynamics

5. FUNDING NUMBERS

WU–505–62–52

6. AUTHOR(S)

K.B.M.Q. Zaman

7. PERFORMING ORGANIZATION NAME(S) AND ADDRESS(ES)

National Aeronautics and Space Administration
Lewis Research Center
Cleveland, Ohio 44135–3191

8. PERFORMING ORGANIZATION REPORT NUMBER

E–9230

9. SPONSORING/MONITORING AGENCY NAME(S) AND ADDRESS(ES)

National Aeronautics and Space Administration
Washington, D.C. 20546–0001

10. SPONSORING/MONITORING AGENCY REPORT NUMBER

NASA TM–106385
AIAA–95–0889

11. SUPPLEMENTARY NOTES

Prepared for the 33rd Aerospace Sciences Meeting and Exhibit sponsored by the American Institute of Aeronautics and Astronautics, Reno, Nevada, January 9–12, 1995. Responsible person, K.B.M.Q. Zaman, organization code 2660, (216) 433–5888.

12a. DISTRIBUTION/AVAILABILITY STATEMENT

Unclassified - Unlimited
Subject Category 02

12b. DISTRIBUTION CODE

13. ABSTRACT (*Maximum 200 words*)

The effects of vortex generators and periodic excitation on vorticity dynamics and the phenomenon of axis switching in a free asymmetric jet are studied experimentally. Most of the data reported are for a 3:1 rectangular jet at a Reynolds number of 450,000 and a Mach number of 0.31. The vortex generators are in the form of "delta tabs", triangular shaped protrusions into the flow, placed at the nozzle exit. With suitable placement of the tabs, axis switching could be either stopped or augmented. Two mechanisms are identified governing the phenomenon. One, as described by previous researchers are referred to here as the ω_θ-*induced dynamics*, is due to difference in induced velocities for different segments of a rolled up azimuthal vortical structure. The other, ω_x-*induced dynamics*, is due to the induced velocities of streamwise vortex pairs in the flow. Both dynamics can be active in a natural asymmetric jet; the tendency for axis switching caused by the ω_θ-induced dynamics may be, depending on the streamwise vorticity distribution, either resisted or enhanced by the ω_x-induced dynamics. While this simple framework qualitatively explains the various observations made on axis switching, mechanisms actually in play may be much more complex. The two dynamics are not independent as the flow field is replete with both azimuthal and streamwise vortical structures which continually interact. Phase averaged flow field data for a periodically forced case, over a volume of the flow field, are presented and discussed in an effort to gain insight into the dynamics of these vortical structures.

14. SUBJECT TERMS

Jets; Vortex dynamics; Mixing; Tabs; Excitation; Flow control

15. NUMBER OF PAGES

18

16. PRICE CODE

A03

17. SECURITY CLASSIFICATION OF REPORT	18. SECURITY CLASSIFICATION OF THIS PAGE	19. SECURITY CLASSIFICATION OF ABSTRACT	20. LIMITATION OF ABSTRACT
Unclassified	Unclassified	Unclassified	